Dynamic average small signal model of the SAB converter

Alexis A. Gómez[1], Alberto Rodríguez[1], Marta M. Hernando[1], Diego G. Lamar[1], Javier Sebastián[1], Ibán Ayarzaguena[2], Jose Manuel Bermejo[2], Igor Larrazabal[2], David Ortega[2], Francisco Vázquez[3]
[1] University of Oviedo,[2] Ingeteam Power Technology S.A., [3] Ingeteam R&D Europe.
[1] Gijón, Spain; [2] Zamudio, Spain; [3] Zamudio, Spain
E-Mail: gomezalexis@uniovi.es
URL: https://sea.grupos.uniovi.es/

Acknowledgements

This work was financed by the European project UE-18-POWER2POWER-826417, by the Principado de Asturias through project SV-PA-21-AYUD/2021/51931, and by the Spanish Ministry of Science, Innovation and Universities through projects MCI-21-PDC2021-121242-I00 and MCI-20-PID2019-110483RB-I00.

Keywords

«Small signal», «Modelling», «Single Active Bridge», «Isolated converter», «DC-DC power converter»

Abstract

In this article the average small signal model of the Single Active Bridge (SAB) converter is obtained. This converter can operate in two different conduction modes, Discontinuous Conduction Mode (DCM) and Continuous Conduction Mode (CCM). The SAB and the Phase-Shifted Controlled Full Bridge (PSFB) converter when operating in DCM present the same static behavior if the value of the inductor of the SAB is the same as the value of the output inductor of the PSFB referred to the primary side of the transformer. This conclusion can be extrapolated from the static analysis to the dynamic average small signal model, as such a first order model is obtained for this operating mode. However, when the SAB converter operates in CCM, the current through the inductor does not start at zero at the beginning of the switching period. Both small signal models are analyzed and confirmed by means of simulations.

Introduction

One of the most common DC-DC bidirectional converters is the Dual Active Bridge (DAB) [1]–[4]. It is an attractive converter for applications in which the power flow is reversible. However, in applications where the power flow is always in the same direction, one port is the input and the other the output, it is possible to substitute the secondary active bridge for a diode H bridge. This converter is referred as the Single Active Bridge (SAB) and although the bidirectional power flow capability is lost due to this change; the power density, reliability and cost are potentially improved. In Fig. 1 a schematic of the SAB converter is shown, and a detailed static analysis is carried out in [5], [6]. Dynamic average small signal modelling of the DAB converter can be found in several publications [3], [4]. The objective of this article is precisely to perform a similar analysis for the SAB converter.

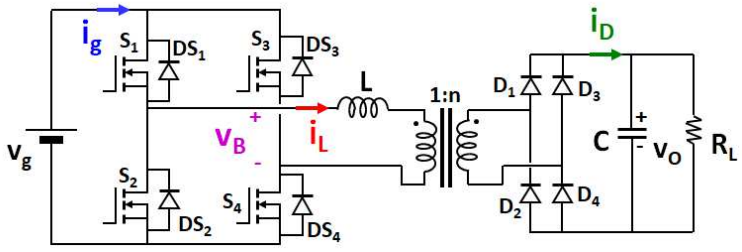

Fig. 1: Single Active Bridge (SAB) converter descriptive schematic

As exposed in [5], [6] the SAB converter can operate in two distinct conduction modes according to the inductor current (i_L) waveform. If the current only crosses and does not remain at zero, the converter operates in Continuous Conduction Mode (CCM), on the contrary if the current level remains at zero as seen in Fig. 2 the converter operates in Discontinuous Conduction Mode (DCM). In Fig. 1, i_D is the injected current into the R_LC net and corresponds to a rectified and scaled version of the current i_L. From this and Fig. 3 it is possible to understand that when the converter operates in DCM the current at the beginning of the switching period is zero. However, when the converter operates in CCM the value at the beginning of the switching period is non zero. This means that in DCM the electrical charge transferred to R_LC is not dependent on the previous switching period as in this mode always ends with no current flowing through the inductor. This implies a cycle-by-cycle update on the transferred power, therefore the resulting dynamic model corresponds to a first order model; similar to other converters, such as the PSFB when operating in DCM. In CCM the current i_L is not always the same at the start of the switching period and depends on the value at the end of the previous switching period. This fact makes for a model of higher order.

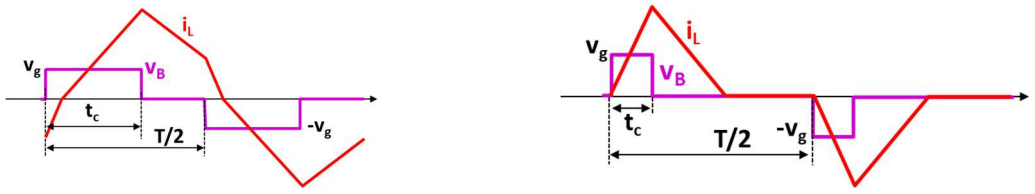

Fig. 2: Current through the inductor i_L and voltage applied to the inductor transformer set. a) in CCM. b) in DCM.

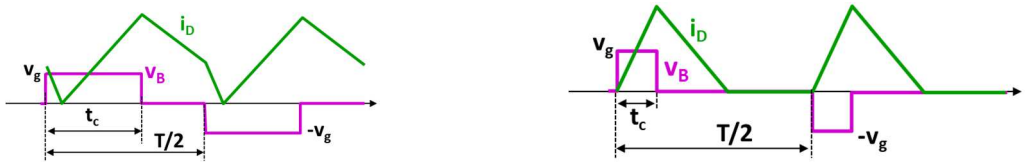

Fig. 3: Current injected to the R_LC net and voltage applied to the inductor transformer set. a) in CCM. b) in DCM.

The method used to obtain the dynamic average small signal models is the Current Injected Equivalent Circuit Approach (CIECA), explained in [7], [8].

Dynamic average small signal model in DCM

The basic idea of CIECA is represented in Fig. 4. The converter shown in Fig. 1 can be divided into three parts: The input voltage source, the set of switches and magnetic elements, and the R_LC output net. The basic idea of CIECA is to substitute the converter for a quadripole composed by two non-linear current sources. These current sources must behave in the same way of the average converter currents they replace. The input current source replaces the average input current, i_{g_avg}. The value of the second current source represents the average current through the secondary diodes bridge, and it is called i_{D_avg}. Therefore, the obtained model possesses the sampling delay characteristic of the averaging process. This delay will only be noticeable when trying to visualize variations close to the switching frequency of the converter, so this effect will be neglected for the model, as it is in most of the other proposed averaged models [7]–[9].

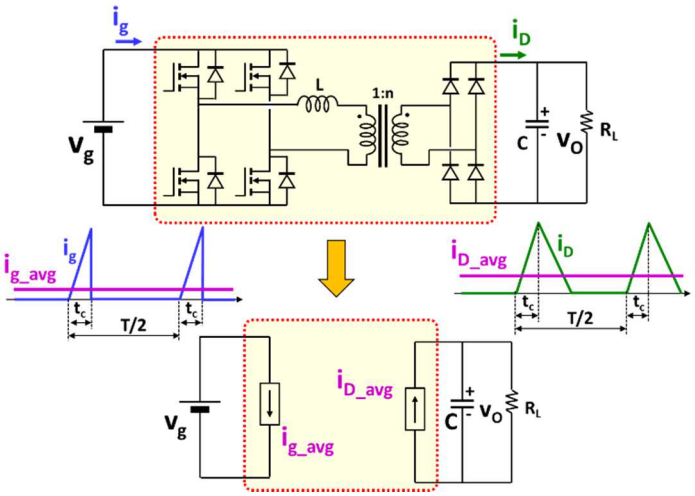

Fig. 4: Process for obtaining an average model using the Current Injected Equivalent Circuit Approach (CIECA).

Considering the waveform of i_D, on [5], [6], and depicted in Fig. 3, (1) was obtained:

$$i_{D\_avg} = \frac{v_g}{LTv_o}\left[v_g - \frac{v_o}{n}\right]t_c^2 \tag{1}$$

Where T is the switching period, L is the inductor, n the transformer relation, v_g is the input voltage, v_o is the output voltage and t_c corresponds to the simultaneous conduction interval of S1 and S4 or S2 and S3, in other words, when + v_g or - v_g is applied to the inductor-transformer arrangement (see Fig. 2 and Fig. 3) in one semi cycle. By conducting a power assessment during a switching period and taking into account that the energy stored on the inductor at the beginning and the end of a switching period is zero, we obtain:

$$I_{g\_avg} = \frac{v_o}{v_g} i_{D\_avg} = \frac{1}{LT}\left[v_g - \frac{v_o}{n}\right]t_c^2 \tag{2}$$

Transforming equations (1) and (2) as functions of the duty cycle, (4) and (5) are obtained. The duty cycle is defined in (3). From (4) and (5) it can be seen that the duty cycle is related to the electrical variables by means of multiplications and divisions, which implies a non-linear model, valid for small and big signal analysis. However, in order to use classic control theory for the feedback loop it is necessary to obtain transfer functions that relate the current sources with the electrical and control variables. To do this a linearization of the current sources around an operating point is carried out using capital letters (D, V_g…). The linearization makes the new model only valid for small signal analysis.

$$d = \frac{t_c}{T} \tag{3}$$

$$i_{D\_avg} = \frac{Tv_g}{Lv_o}\left[v_g - \frac{v_o}{n}\right]d^2 \tag{4}$$

$$i_{g\_avg} = \frac{T}{L}\left[v_g - \frac{v_o}{n}\right]d^2 \tag{5}$$

The linearization process transforms the quadripole from Fig. 4 into the one shown in Fig. 5. In this figure the variables represented by capital letters are associated with the operating point, whereas the ones with a circumflex accent correspond to the small signal perturbations.

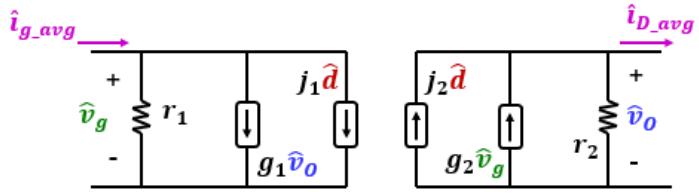

$$\frac{1}{r_1} = \frac{\partial i_{g\_avg}}{\partial v_g}\Big]_{\hat{v}_O=\hat{d}=0} \quad g_1 = \frac{\partial i_{g\_avg}}{\partial v_O}\Big]_{\hat{d}=\hat{v}_g=0} \quad j_1 = \frac{\partial i_{g\_avg}}{\partial d}\Big]_{\hat{v}_O=\hat{v}_g=0} \qquad j_2 = \frac{\partial i_{D\_avg}}{\partial d}\Big]_{\hat{v}_O=\hat{v}_g=0} \quad g_2 = \frac{\partial i_{D\_avg}}{\partial v_g}\Big]_{\hat{v}_O=\hat{d}=0} \quad \frac{1}{r_2} = -\frac{\partial i_{D\_avg}}{\partial v_O}\Big]_{\hat{d}=\hat{v}_g=0}$$

Fig. 5: Small signal canonical circuit.

If the control variable is the duty cycle, the different transfer functions can be calculated as:

$$G_{od} = \frac{\widehat{v_o}}{\hat{d}}\Big|_{\widehat{v_g}=0} = \frac{j_2 R_{eq}}{1 + R_{eq} C s} \tag{6}$$

$$G_{og} = \frac{\widehat{v_o}}{\widehat{v_g}}\Big|_{\hat{d}=0} = \frac{g_2 R_{eq}}{1 + R_{eq} C s} \tag{7}$$

Where:

$$R_{eq} = \frac{R_L r_2}{R_L + r_2} = \frac{V_o(1-N)}{I_o(2-N)} \tag{8}$$

$$j_2 R_{eq} = \frac{2}{nN(2-N)} \sqrt{\frac{[V_o(1-N)]^3}{I_o L f}} \tag{9}$$

$$g_2 R_{eq} = nN \tag{10}$$

$$N = \frac{V_o}{nV_g} \tag{11}$$

As anticipated, G_{od} and G_{og} are first order transfer functions with a pole in the negative semi-plane. A comparative analysis with the transfer functions obtained by means of an analogue analysis of the PSFB converter when operating in DCM would reveal the same equations with the value of L transferred to the other side of the transformer. The parameters for both transfer functions are summarized in Table . Two equivalent equation formats are provided in Table I, the first uses the duty cycle, whereas the second uses external magnitudes.

Table I: Parameter values of the averaged small signal canonical circuit in DCM.

Parameter	j_1	g_1	r_1	j_2	g_2	r_2
Form 1	$\frac{2TD}{L}\left[V_G - \frac{V_o}{n}\right]$	$-\frac{TD^2}{nL}$	$\frac{L}{TD^2}$	$\frac{2TV_gD}{LV_o}\left[V_g - \frac{V_o}{n}\right]$	$\frac{TD^2}{L}\left[\frac{2V_g}{V_o} - \frac{1}{n}\right]$	$\frac{LV_o^2}{TD^2V_g^2}$
Form 2	$2\sqrt{I_o}\sqrt{\frac{V_o(1-N)}{Lf}}$	$-I_o\frac{nN^2}{V_o(1-N)}$	$\frac{V_o(1-N)}{n^2N^2I_o}$	$\frac{2\sqrt{I_o}}{nN}\sqrt{\frac{V_o(1-N)}{Lf}}$	$\frac{NnI_o(2-N)}{V_o(1-N)}$	$\frac{V_o(1-N)}{I_o}$

Dynamic average small signal model in CCM

As stated before, when the SAB converter operates in CCM the transferred electrical charge from the secondary diode bridge to the R_LC network during a switching period it is not independent from the previous switching periods. This is because the current through the inductor does not start at zero, as it did for DCM. Therefore, the area under the current waveform, the transferred charge, will depend on the starting current value. It is clear then that a change of the control variable does not determine the

final transferred charge value during the next switching period, and it is logical to assume that several periods are necessary for the transferred charge on each switching period to settle on the stationary value. The number of cycles necessary to reach steady state will be obtained through simulations and if this effect can or cannot be deemed negligible.

Assuming that the change of the control variable results on a change of the transferred charge value during the next switching period equal to the steady state value, the same process applied to DCM can be used for CCM. The equations for the average input and secondary side diodes currents in CCM are (12) and (13).

$$i_{D\_avg} = \frac{T}{2Ln}\left[v_g d - v_g d^2 - \frac{v_o^2}{4n^2 v_g}\right] \tag{12}$$

$$i_{g\_avg} = \frac{T}{2Ln}\left[v_o d - v_o d^2 - \frac{v_o^3}{4n^2 v_g^2}\right] \tag{13}$$

The linearization process results in the same canonical circuit of Fig. 5. However, on this occasion, the parameters are those of Table II and Table III. The transfer functions can be expressed as before in (6) and (7) with the new parameters from Table and Table . As r_2 changed, the value of R_{eq} also changed. The value of $j_2 R_{eq}$ does not coincide with (9), but $g_2 R_{eq}$ does correspond with (10). A comparison between the different parameters of both conduction modes when operating at the border from each mode is carried out in Table IV, the equations obtained consider border mode operating point, therefore $2nD = V_o/V_g$. From this table, parameters of the canonical circuit differ from one conduction mode to another, creating an abrupt change at the border between conduction modes.

Table II: Parameter values of the averaged small signal canonical circuit in CCM. Primary side.

Parameter	j_1	g_1	r_1
Form 1	$\frac{TV_o}{2Ln}(1-2D)$	$\frac{T}{2nL}\left[D(1-D) - \frac{3}{4n^2}\left(\frac{V_g}{V_o}\right)^2\right]$	$\frac{4n^3L}{T}\left(\frac{V_g}{V_o}\right)^3$
Form 2	$\frac{V_o}{2Lfn}\sqrt{1 - N^2 - \frac{8NLn^2 f I_o}{V_o}}$	$\frac{I_o Nn}{V_o} - \frac{N^2}{4Lfn}$	$\frac{4Lf}{N^3}$

Table III: Parameter values of the averaged small signal canonical circuit in CCM. Secondary side.

Parameter	j_2	g_2	r_2
Form 1	$\frac{TV_g}{2nL}(1-2D)$	$\frac{T}{2nL}\left[D(1-D) + \frac{1}{4n^2}\left(\frac{V_o}{V_g}\right)^2\right]$	$\frac{4n^3L}{T}\left(\frac{V_g}{V_o}\right)$
Form 2	$\frac{V_o}{2Lfn^2N}\sqrt{1 - N^2 - \frac{8NLn^2 f I_o}{V_o}}$	$\frac{I_o nN}{Vo} + \frac{N^2}{4Lfn}$	$\frac{4Lfn^2}{N}$

Table IV: Parameter values of the canonical circuits at both sides of the operation modes border.

Parameter	j_1	g_1	r_1	j_2	g_2	r_2
DCM	$\frac{TV_o}{nL}(1-N)$	$-\frac{TN^2}{4nL}$	$\frac{4L}{TN^2}$	$\frac{TV_o}{n^2NL}(1-N)$	$\frac{TN}{4nL}(2-N)$	$\frac{4n^2L}{T}$
CCM	$\frac{TV_o}{2nL}(1-N)$	$\frac{TN}{4nL}(1-2N)$	$\frac{4L}{TN^3}$	$\frac{TV_o}{2n^2NL}(1-N)$	$\frac{TN}{4nL}$	$\frac{4n^2L}{TN}$

Simulation results

In order to check the theoretical model, a PSIM simulation has been done of a converter designed using the design guide presented on [5], [6]. The resulting converter designed in [5] can be defined by f=100 kHz, n=0.55, L=78.96 µH. All the semiconductors are considered ideal, the magnetizing inductance is 789.6 mH and no transformer leakage inductance is considered.

With this converter, the parameter values are evaluated for two operating points, one in DCM and other in CCM, but near the border as one of the most important characteristics is the change in the parameters. The nominal input and output voltages are V_g= 400 V and V_o= 44 V. Using (11) this means a value of N=0.2. Knowing that the normalized voltage conversion ratio at the border between CCM and DCM is $N=2D_{crit}$, the critical duty cycle is D_{crit}=0.1. The chosen duty cycles are slightly under 0.1 for DCM and slightly above for CCM.

To calculate the canonical circuit parameters from the simulations, denoted by the suffix sim, the following expressions are used.

$$r_{1\ sim} = \frac{V_{g\,2} - V_{g\,1}}{I_{g\ avg\,sim}(V_{g\,2}) - I_{g\ avg\,sim}(V_{g\,1})} \tag{14}$$

$$g_{1\,sim} = \frac{I_{g\,avg\,sim}(V_{o\,2}) - I_{g\,avg\,sim}(V_{o\,1})}{V_{o\,2} - V_{o\,1}} \tag{15}$$

$$j_{1\,sim} = \frac{I_{g\,avg\,sim}(D_2) - I_{g\,avg\,sim}(D_1)}{D_2 - D_1} \tag{16}$$

To calculate r_1 the variation of average input current is observed when the input voltage changes, while maintaining the output voltage and duty cycle constant. For g_2 is the output voltage that suffers a variation, while maintaining the input voltage and duty cycle fixed. Finally, j_1 is calculated by observing the change in input average current when the duty cycle varies. To calculate the second side parameters, the same equations can be used by substituting the first side parameters for the second side and vice versa.

For this the simulated circuit corresponds to that of Fig. 1. To calculate j_1 and j_2 the input and output voltages are kept at nominal values, whereas the duty cycle changes from 0.090 to 0.100 for DCM and from 0.105 to 0.115 for CCM. For r_1 and g_2 the input voltage varies from 390 V to 400 V. And for g_1 and r_2 the output voltage varies from 44 V to 46 V. The nominal duty cycle values are 0.10 for DCM and 0.11 for CCM.

Theoretical and simulations results for all the parameters in both conduction modes are compared in Table IV. As shown, theoretical results exhibit a good correlation with simulation values.

Table V: Comparison of theoretical and simulation of canonical circuit parameters.

Parameters in CCM	j_1 (A)	g_1 (Ω^{-1})	r_1 (Ω)	j_2 (A)	g_2 (Ω^{-1})	r_2 (Ω)
Theoretical	4.05	0.0069	3953.6	36.8	0.0115	47.8
Simulated	4.15	0.0076	5000.0	37.0	0.0120	50.0

Parameters in DCM	j_1 (A)	g_1 (Ω^{-1})	r_1 (Ω)	j_2 (A)	g_2 (Ω^{-1})	r_2 (Ω)
Theoretical	8.11	-0.0023	789.9	73.7	0.0207	9.6
Simulated	7.40	-0.0021	909.1	66.00	0.0180	10.5

In order to confirm the validity of the first order model approximation when the converter operates in CCM, Bode diagrams of the G_{od} transfer functions for both conduction modes are represented in Fig. 6,

these graphs were obtained by simulating the full switching circuit with a sinusoidal perturbation. These graphs show an almost perfect correlation between theoretical and simulation results for DCM, and a very good approximation for CCM. This confirms the initial assumption, the dynamic CCM model can be approximated as a first order model. A theoretical (G_{od}) and simulation step response of the output voltage when the duty cycle changes is depicted in Fig. 7. Fig. 7 a) corresponds when the converter operates in CCM, the duty cycle changes from 0.11 to 0.13. Fig. 7 b) does the same for DCM, the duty cycle changes from 0.077 to 0.097.

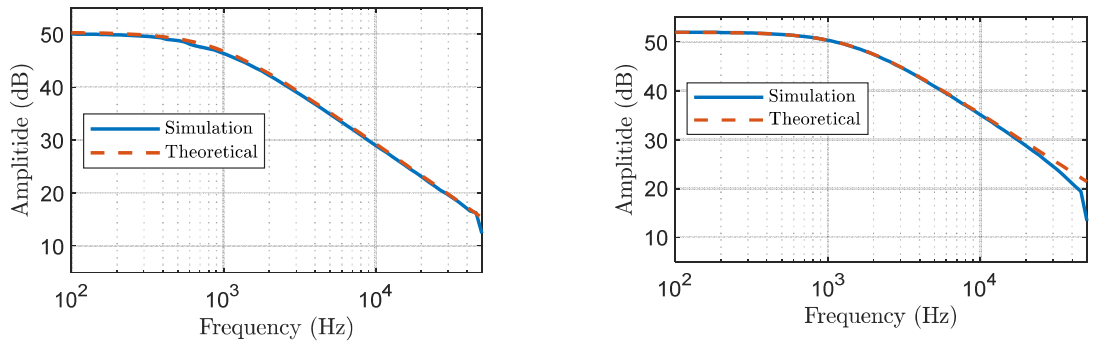

a) b)

Fig. 6: Amplitude Bode diagrams of the transfer function G_{od} a) in CCM. b) in DCM.

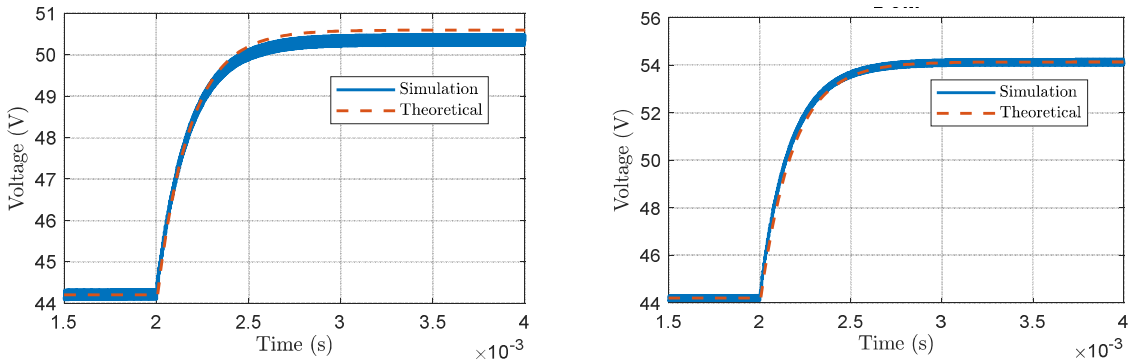

a) b)

Fig. 7: Step response of the output voltage to a change in the duty cycle. a) in CCM. b) in DCM.

If the converter is subject to the same duty cycles steps as before but maintaining the input and output voltages constant, at 400 V and 44 V respectively; the current through the inductor and the diodes bridge changes instantly, when the converter operates in DCM. However, if the converter is working on CCM the change does not happen instantly and the current oscillates for a few cycles. In Fig. 8, the current through the secondary diode bridge is represented when the duty cycle changes from 0.77 to 0.97 in DCM and 0.11 to 0.13 in CCM while maintaining the input and output voltages.

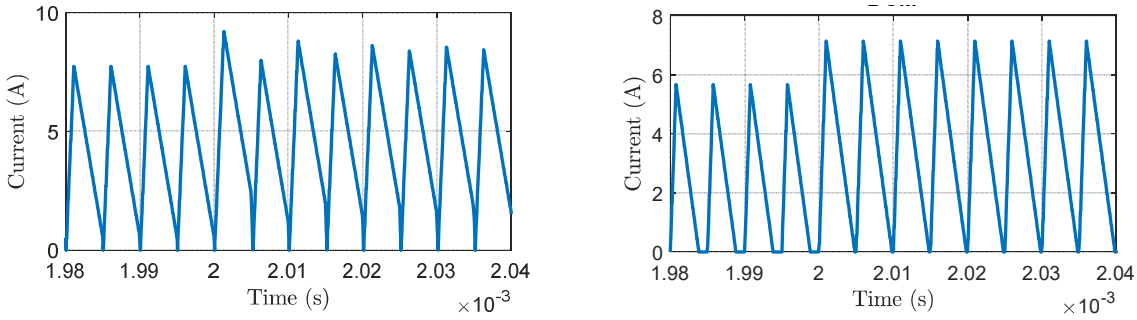

a) b)

Fig. 8: Step response of the current through the secondary diode bridge. a) in CCM. b) in DCM.

Conclusion

This article provides a dynamic average small signal model of the SAB converter. With the obtained results it is possible to assume a first order model for either operation mode DCM or CCM. Linearized small signal models are presented for DCM and CCM, as well as transfer functions between duty cycle and output voltage perturbations, and input and output voltages perturbations; both necessary to design a control loop. Parameters of these models are found to be different at different sides of the border between CCM and DCM. This is not a surprising fact, as it happens in the case of other converters.

References

[1] R. W. A. A. De Doncker, D. M. Divan, and M. H. Kheraluwala, "A three-phase soft-switched high-power-density DC/DC converter for high-power applications," *IEEE Transactions on Industry Applications*, vol. 27, no. 1, pp. 63–73, Jan. 1991, doi: 10.1109/28.67533.

[2] M. N. Kheraluwala, R. W. Gascoigne, D. M. Divan, and E. D. Baumann, "Performance characterization of a high-power dual active bridge DC-to-DC converter," *IEEE Transactions on Industry Applications*, vol. 28, no. 6, pp. 1294–1301, Nov. 1992, doi: 10.1109/28.175280.

[3] A. R. Rodríguez Alonso, J. Sebastian, D. G. Lamar, M. M. Hernando, and A. Vazquez, "An overall study of a Dual Active Bridge for bidirectional DC/DC conversion," in *2010 IEEE Energy Conversion Congress and Exposition*, Sep. 2010, pp. 1129–1135. doi: 10.1109/ECCE.2010.5617847.

[4] A. Rodríguez, A. Vázquez, D. G. Lamar, M. M. Hernando, and J. Sebastián, "Different Purpose Design Strategies and Techniques to Improve the Performance of a Dual Active Bridge With Phase-Shift Control," *IEEE Transactions on Power Electronics*, vol. 30, no. 2, pp. 790–804, Feb. 2015, doi: 10.1109/TPEL.2014.2309853.

[5] F. J. Sebastián *et al.*, "Estudio estático completo del convertidor Single Active Bridge," *Seminario Anual de Automática, Electrónica industrial e Instrumentación (SAAEI)*, 2021, Accessed: Feb. 16, 2022. [Online]. Available: https://digibuo.uniovi.es/dspace/handle/10651/60273

[6] A. Rodriguez *et al.*, "An Overall Analysis of the Static Characteristics of the Single Active Bridge Converter," *Electronics*, vol. 11, no. 4, Art. no. 4, Jan. 2022, doi: 10.3390/electronics11040601.

[7] P. R. K. Chetty, "Current Injected Equivalent Circuit Approach to Modeling of Switching DC-DC Converters in Discontinuous Inductor Conduction Mode," *IEEE Transactions on Industrial Electronics*, vol. IE-29, no. 3, pp. 230–234, Aug. 1982, doi: 10.1109/TIE.1982.356670.

[8] P. R. K. Chetty, "CIECA: Application to Current Programmed Switching Dc-Dc Converters," *IEEE Transactions on Aerospace and Electronic Systems*, vol. AES-18, no. 5, pp. 538–544, Sep. 1982, doi: 10.1109/TAES.1982.309266.

[9] S. Cuk and R. D. Middlebrook, "A general unified approach to modelling switching DC-tO-DC converters in discontinuous conduction mode," in *1977 IEEE Power Electronics Specialists Conference*, Jun. 1977, pp. 36–57. doi: 10.1109/PESC.1977.7070802.